JACS
JOURNAL OF THE AMERICAN CHEMICAL SOCIETY
Article
pubs.acs.org/JACS

Photocleavable Hydrogel-Coated Upconverting Nanoparticles: A Multifunctional Theranostic Platform for NIR Imaging and On-Demand Macromolecular Delivery

Ghulam Jalani,[‡] Rafik Naccache,[†] Derek H. Rosenzweig,[§] Lisbet Haglund,[§] Fiorenzo Vetrone,*[,†] and Marta Cerruti*[,‡]

[‡]Department of Mining and Materials Engineering, McGill University, Montreal, QC H3A 0C5, Canada

[†]Institut National de la Recherche Scientifique-Énergie, Matériaux et Télécommunications, Université du Québec, Varennes, QC J3X 1S2, Canada

[§]Department of Surgery, McGill University, Montreal, QC H3G 1A4, Canada

Supporting Information

ABSTRACT: Lanthanide-doped upconverting nanoparticles (UCNPs) have emerged as excellent nanotransducers for converting longer wavelength near-infrared (NIR) light to shorter wavelengths spanning the ultraviolet (UV) to the visible (Vis) regions of the spectrum via a multiphoton absorption process, known as upconversion. Here, we report the development of NIR to UV−Vis−NIR UCNPs consisting of $LiYF_4$:Yb^{3+}/Tm^{3+}@SiO_2 individually coated with a 10 ± 2 nm layer of chitosan (CH) hydrogel cross-linked with a photocleavable cross-linker (PhL). We encapsulated fluorescent-bovine serum albumin (FITC-BSA) inside the gel. Under 980 nm excitation, the upconverted UV emission cleaves the PhL cross-links and instantaneously liberates the FITC-BSA under 2 cm thick tissue. The release is immediately arrested if the excitation source is switched off. The upconverted NIR light allows for the tracking of particles under the tissue. Nucleus pulposus (NP) cells cultured with UCNPs are viable both in the presence and in the absence of laser irradiation. Controlled drug delivery of large biomolecules and deep tissue imaging make this system an excellent theranostic platform for tissue engineering, biomapping, and cellular imaging applications.

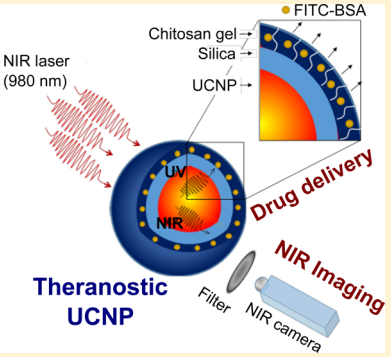

INTRODUCTION

On-demand drug delivery using stimuli-responsive hydrogels is useful for local and recurring therapies such as in the treatment of localized infections, solid tumors, and postsurgical wounds, because it minimizes side effects associated with anesthetics, antibiotics, and anticancer therapeutic agents.[1,2] A stimulus applied externally (e.g., temperature, light, ultrasound, electrical, or magnetic field), or generated in situ (e.g., pH change or presence of enzymes), induces a physical or chemical change in the polymeric structure of the hydrogel, triggering the release of the encapsulated cargo.[3] External stimuli allow for a better control of the time and dosage of released drugs,[4,5] and among externally controlled stimuli, light offers many advantages such as noninvasiveness, high temporal resolution, and the ability to be controlled remotely with relatively high local precision.[1,6] In light-controlled systems, a photoactive molecule undergoes a change in its physical or chemical structure when exposed to light of a specific wavelength, triggering the delivery process.[7]

Several photoresponsive molecules have been developed.[8] An example is azobenzene, which undergoes photoisomerization when exposed to UV light, readily changing its orientation from "extended" to "bent".[9,10] This property has been exploited to transform azobenzene molecules into flexible propellers anchored inside polymeric micelles and mesoporous silica nanoparticles for photoregulated delivery of doxorubicin.[11] Another group of photoactive molecules contains *o*-nitrobenzyl moieties in their structure and an ester bond, which is irreversibly cleaved when irradiated with UV light.[12] They can be further modified to introduce reactive sites on their structure for conjugation with drugs or biomolecules.[13,14]

Although photocontrolled drug delivery provides several advantages over other stimuli-responsive systems,[15,16] there is a severe limitation associated with the use of light-controlled systems in vivo: UV light is required for most of the photoreactions to occur.[17] However, UV light cannot deeply penetrate inside the body, because it is largely absorbed by the skin and underlying fat tissues.[18] This leads to inefficient photoreactions and poor control over drug release. In addition, UV light is carcinogenic, and under prolonged exposure, it can induce tissue damage. Both of these factors limit the use of UV light as a trigger for in vivo applications. In contrast, NIR light can achieve deep penetration in the body (up to 3.2 cm), because biological tissues are transparent to NIR wavelengths.[19] However, NIR light cannot be directly used because most of the photoreactions require high energy UV or visible light to

Received: December 2, 2015
Published: December 27, 2015

DOI: 10.1021/jacs.5b12357
J. Am. Chem. Soc. 2016, 138, 1078−1083

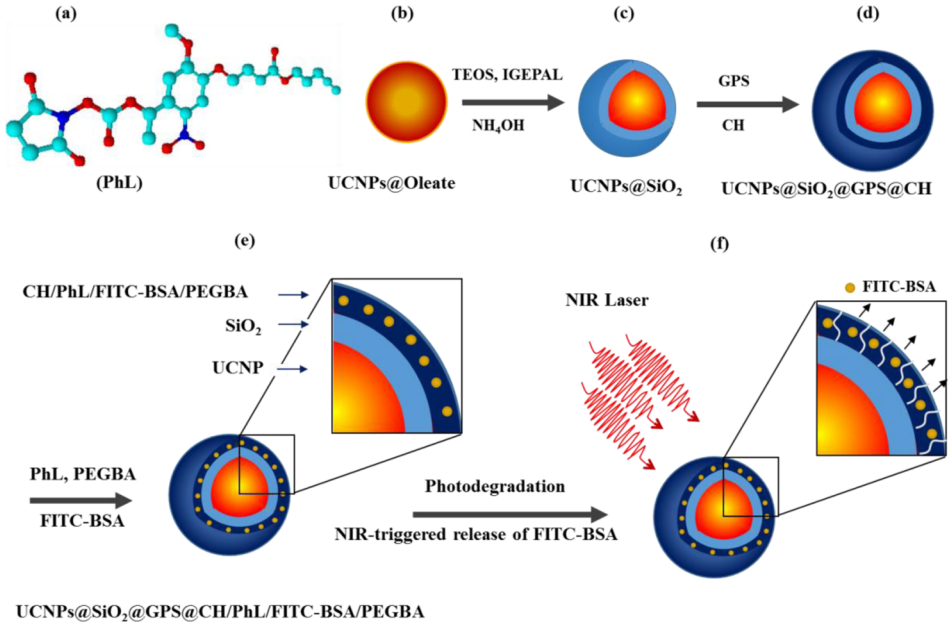

Figure 1. Schematic illustration of the synthesis of photodegradable hydrogel-coated UCNPs and drug release mechanism. (a) Chemical structure of PhL containing acetylene and succinimidyl group on two ends, (b) oleate-capped UCNPs, (c) SiO_2-coated UCNPs, (d) GPS and CH modified UCNPs, (e) PhL/PEGBA-cross-linked UCNPs@GPS@SiO_2@CH encapsulating FITC-BSA molecules inside the CH shell, and (f) NIR-triggered photodegradation and drug release.

occur.[20] The ideal solution to this problem is thus to generate UV light in situ via a transducer that can upconvert NIR to UV radiation in situ.

Lanthanide-doped UCNPs have been developed to act as these transducers. UCNPs can convert longer wavelength NIR radiation (typically 800 or 980 nm) to shorter wavelength UV, Vis, and NIR radiation, thanks to the presence of multiple long-lived 4f electronic states, equally spaced in a ladder-like configuration, which allow two (or more) low energy photons to be sequentially absorbed and converted to a higher energy photon.[21−23] UCNPs have been used for NIR-triggered anticancer drug delivery from hydrogels, block copolymer micelles,[24] and mesoporous silica nanoparticles,[11] using azobenzene or *o*-nitrobenzyl as photoactive molecules.[25] Recently, Yan et al. designed a phototriggered drug delivery system consisting of polyethylene glycol-acrylamide hydrogels cross-linked with a modified *o*-nitrobenzyl linker and mixed with UCNPs for NIR-regulated release of biomacromolecules.[26] However, high laser power and long irradiation time were required to degrade the hydrogel and release the drug. This was due to the limited efficiency of the photocleavage in this system: the upconverted UV light had to travel through the whole hydrogel to reach all photocleavable cross-links.

We have previously shown that $LiYF_4$ UCNPs doped with Yb^{3+} and Tm^{3+} ions produce multiple emissions spanning UV, Vis, and NIR regions.[27] In particular, intense UV emissions at 347 and 362 nm are observed along with a strong NIR band at 790 nm. We have also shown that the upconverted NIR band at 790 nm can be used for deep tissue imaging of live intervertebral discs.[28] Here, we individually coat these UCNPs with a thin shell of CH, entrap FITC-BSA molecules, and cross-link the shell with a photocleavable cross-linker. Upon NIR irradiation (980 nm), the upconverted UV emission from UCNPs cleaves the cross-linked CH chains, resulting in instantaneous liberation of encapsulated FITC-BSA.

RESULTS AND DISCUSSION

Figure 1 shows a schematic of the experimental design used to develop the drug delivery system. At the onset, we synthesized the photocleavable cross-linker (PhL) containing a succinimidyl group on one end and an acetylene group on the other end (Figure 1a). A schematic of PhL synthesis is given in Figure S1, and its NMR spectrum is given in Figure S2. To produce photodegradable CH hydrogel-coated UCNPs, we synthesized oleate-capped UCNPs (UCNPs@Oleate) (Figure 1b), composed of $LiYF_4$:Yb^{3+}/Tm^{3+}, using the thermal decomposition method. These hydrophobic UCNPs were rendered hydrophilic by coating with a thin shell of SiO_2 (UCNPs@SiO_2) (Figure 1c). We used (3-glycidyloxypropyl) trimethoxysilane (GPS) to introduce epoxy groups on the surface of UCNPs@SiO_2 (UCNPs@SiO_2@GPS) and incubated the resulting particles with a CH solution, allowing the amino groups from the latter to readily react with the epoxide groups present on UCNPs@SiO_2@GPS, thus yielding CH-modified UCNPs (UCNPs@SiO_2@GPS@CH) (Figure 1d). We then reacted the succinimidyl groups present on one end of the PhL with residual amino groups on CH chains to produce PhL-modified UCNPs (UCNPs@SiO_2@GPS@CH/PhL), and entrapped FITC-BSA molecules between the flexible CH chains (UCNPs@SiO_2@GPS@CH@PhL/FITC-BSA). Finally, we introduced polyethylene glycol-bisazide (PEGBA) to complete the cross-linking by reacting the azide groups from PEGBA with the acetylene groups present on the free ends of PhL, via a click reaction (UCNPs@SiO_2@GPS@CH/PhL/FITC-BSA/PEGBA) (Figure 1e). The chemistry of the final construct is shown in Figure S3. Upon irradiation with a 980 nm laser, several processes are expected to occur. First, the UCNPs upconvert the incident NIR light to UV light. Second, the PhL absorbs the UV radiation and is photocleaved, thus breaking the cross-links that hold together the CH shell. Last, the hydrogel is partially dissociated, and FITC-BSA molecules are liberated (Figure 1f).

DOI: 10.1021/jacs.5b12357
J. Am. Chem. Soc. 2016, 138, 1078−1083

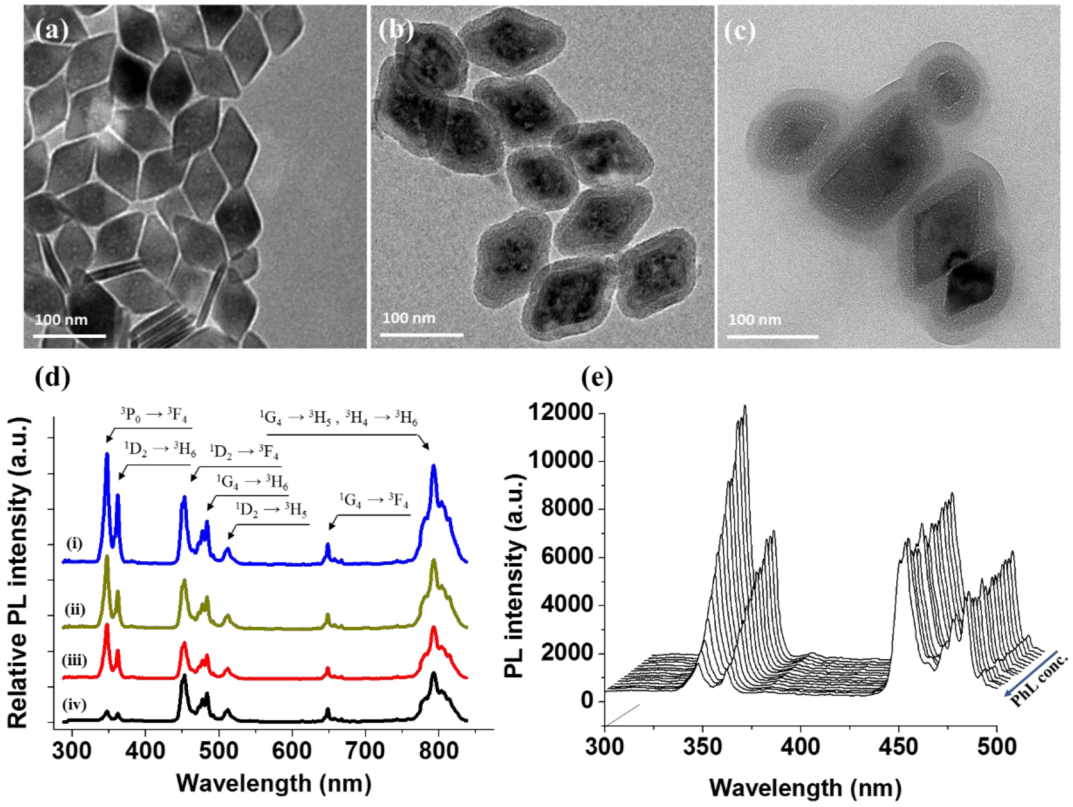

Figure 2. TEM images of (a) oleate-capped UCNPs, (b) UCNPs@SiO_2, and (c) UCNPs@SiO_2@GPS@CH/PhL/FITC-BSA/PEGBA showing homogeneously dispersed UCNPs. (d) Overlayed upconversion PL spectra of UCNPs (i), UCNPs@SiO_2 (ii), UCNPs@SiO_2@GPS@CH (iii), and UCNPs@SiO_2@GPS@CH/PhL/PEGBA (iv). (e) Upconversion PL spectra of UCNPs@SiO_2@GPS@CH/PEGBA cross-linked with variable amounts of PhL ranging from 0 to 75 μM.

To confirm the successful surface modification of the UCNPs, we used X-ray photoelectron spectroscopy (XPS) to probe the surface following each step. High-resolution C_{1s}, Si_{2p}, and N_{1s} spectra are shown in Figure S4 and confirm the successful modification of the UCNPs with SiO_2, GPS, and CH. Successful modification of the UCNP surface was also evidenced by transmission electron microscopy (TEM) as shown in Figure 2a where uniformly distributed oleate-capped UCNPs with an average length, width, and thickness of 78 ± 6, 52 ± 8, and 7 ± 2 nm, respectively, were observed. Following modification with SiO_2, an 8 ± 2 nm thick shell was observed around each UCNP (Figure 2b). Figure 2b also shows that all UCNPs were individually coated, and no aggregation during the SiO_2 coating process was observed. After GPS modification, CH attachment, and cross-linking with PhL, an additional shell 10 ± 3 nm in thickness was observed, pointing to the presence of a layer of the CH hydrogel around each particle (Figure 2c). The hydrogel coating was uniform around all UCNPs@SiO_2 with no significant aggregation observed.

The upconversion PL emission spectra of the UCNPs, UCNPs@SiO_2, UCNPs@SiO_2@GPS@CH, and UCNPs@SiO_2@GPS@CH/PhL/PEGBA were recorded to evaluate the effect of SiO_2, CH, and PhL on the emission of UCNPs (Figure 2d). The PL spectrum of 1 w/v % suspension of UCNPs (in hexane) showed two strong UV emission peaks at 347 and 362 nm, corresponding to the $^3P_0 \rightarrow {}^3F_4$ and $^1D_2 \rightarrow {}^3H_6$ transitions, respectively, four visible emission peaks at 450, 482, 512, and 649 nm, corresponding to the $^1D_2 \rightarrow {}^3F_4$, $^1G_4 \rightarrow {}^3H_6$, $^1D_2 \rightarrow {}^3H_5$, and $^1G_4 \rightarrow {}^3F_4$ transitions, and an intense NIR peak at 791 nm, ascribed to the $^1G_4 \rightarrow {}^3H_5$ and $^3H_4 \rightarrow {}^3H_6$ transitions, respectively (Figure 2d (i)).[27,29] The PL spectra of UCNPs@SiO_2 (Figure 2d (ii)) and UCNPs@SiO_2@GPS@CH (Figure 2d (iii)) showed similar yet less intense peaks. The lower intensity could be due to the quenching effect of the SiO_2 and CH shells present around the UCNPs and their associated large vibrational energies. The PL spectrum of UCNPs@SiO_2@GPS@CH/PhL/PEGBA (Figure 2d (iv)) showed emission peaks at the same positions as those observed for the other UCNPs samples; however, the incorporation of PhL selectively quenched the UV emission bands (347 and 362 nm), thus suggesting that the upconverted UV light was efficiently absorbed by the PhL present in the CH shell. This result can be explained by the excellent match between the absorption spectrum of the PhL and the emission spectrum of the UCNPs (Figure S5a): the main absorption peak of PhL is centered at 348 nm, which overlaps the UV emission peak of UCNPs@SiO_2, thus explaining the selective absorption of the UV emissions observed in Figure 2d (iv).

We investigated the effect of the PhL on the emission of UCNPs@SiO_2 by cross-linking the CH shell with variable amounts of PhL and recorded the corresponding emission spectra under 980 nm laser irradiation. The spectra in Figure 2e showed that the quenching of the UV emission is dependent on the amount of PhL added. This is quantified in Figure S5b, where the intensity of the 347 nm peak in the PL spectra of UCNPs@SiO_2@GPS@CH/PhL/PEGBA was plotted as a function of PhL concentration. The intensity of the 347 nm emission decreases linearly (R^2 = 0.998) as the concentration of PhL is increased from 0 to 75 μM, again showing that UV light is efficiently absorbed by the PhL and confirming that the

DOI: 10.1021/jacs.5b12357
J. Am. Chem. Soc. 2016, 138, 1078−1083

quenching of UV band observed earlier in Figure 2d (iv) was due to the presence of PhL. To determine if UV light absorption actually cleaves the PhL and thus degrades the CH shell around the UCNPs, we recorded the UV−Vis absorption spectra of UCNPs@SiO_2@GPS@CH/PhL/PEGBA before and after irradiation with NIR laser (Figure S6a). Prior to irradiation, three distinct peaks were observed in the UV region centered at 346, 302, and 245 nm. After irradiation, the position of the peaks at 346 and 302 nm remained unchanged, while the peak at 245 nm split into three peaks centered at 201, 221, and 245 nm, indicating a change in the chemical structure of PhL. To confirm that the PhL cross-linked to the CH shell is released upon UV absorption, we recorded the UV−Vis spectra of the supernatant solution, obtained following irradiation of the UCNPs and their isolation using centrifugation (Figure S6b). The background signal of the supernatant prior to irradiation (0 min) does not show any peak; however, following irradiation, all spectra showed peaks between 200 and 250 nm, similar to those observed in the absorption spectra of the photocleaved PhL molecules (Figure S6a, red line), which confirms the successful release of the photocleaved PhL. The intensity of all peaks gradually increased with irradiation time, indicating a gradual loss of PhL cross-links from the CH shell.

After confirming that NIR light can be used to successfully photocleave the cross-linked PhL in the CH shell, we encapsulated FITC-BSA as a model macromolecular drug (UCNPs@SiO_2@GPS@CH/PhL/FITC-BSA/PEGBA). The FITC-BSA was added prior to the final cross-linking step with PEGBA, and we monitored its release under NIR irradiation, using UV−Vis spectroscopy. The UV−Vis absorption spectra of the supernatant solution collected after irradiation and isolation of the particles (Figure 3a) showed a mixture of peaks due to the presence of FITC-BSA (i) and PhL (ii), indicating that both are simultaneously released. The spectral intensity increased as the irradiation time was increased from 2 to 8 min, similarly to what was previously observed (Figure S6b).

The effect of laser power and irradiation time on the release of FITC-BSA is shown in Figure 3b: UCNPs@SiO_2@GPS@CH/PhL/FITC-BSA/PEGBA were irradiated for different times under different laser powers, centrifuged, and the cumulative amount of FITC-BSA released in the supernatant was measured using UV−Vis spectroscopy. The plots in Figure 3b show a linear increase in the release of FITC-BSA up to 9 min of irradiation at a laser power density of 1.8 W/cm^2; this linear region extends to 12 min at laser power densities of 1.5 and 1.2 W/cm^2. These results show that the gradual loss of cross-links and degradation of the CH shell with irradiation time causes a gradual release of the encapsulated drug. The plateau observed after 9 min of irradiation at a laser power density of 1.8 W/cm^2, at ∼92% of the initially loaded FITC-BSA, shows that in this condition most of the cross-links inside the CH shell take 9 min to be broken. The lack of a plateau region at lower power densities indicates that under these conditions the CH shell is not completely degraded even after 12 min of irradiation.

To evaluate the on-demand drug release ability of this system, we irradiated UCNPs@SiO_2@GPS@CH/PhL/FITC-BSA/PEGBA with the NIR laser at 1.8 W/cm^2. The laser was switched on for 1 min and then switched off for 50 min during which time we monitored the FITC-BSA release. The results shown with red and blue dots in Figure 3c show that in the absence of laser irradiation, no FITC-BSA was released, except

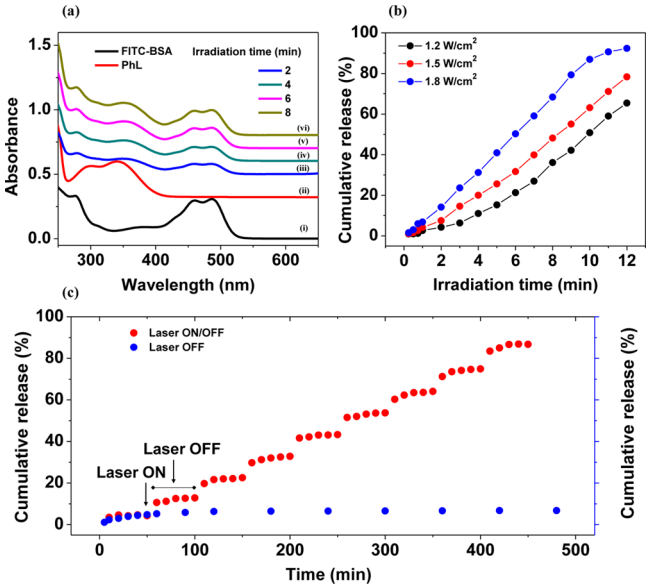

Figure 3. (a) UV−Vis absorption spectra of FITC-BSA (i), PhL (ii), and PhL/PEGBA/FITC-BSA segments ((iii)−(vi)) released under NIR irradiation of UCNPs@SiO_2@GPS@CH/PhL/FITC-BSA/PEGBA. (b) Cumulative FITC-BSA release from UCNPs@SiO_2@GPS@CH/PhL/FITC-BSA/PEGBA as a function of irradiation time at different laser powers. (c) Cumulative FITC-BSA release from UCNPs@SiO_2@GPS@CH/PhL/FITC-BSA/PEGBA as a function of time in the absence of laser irradiation (blue ●) and under periodic irradiation with NIR laser (red ●). The laser ON/OFF cycles are 1/50 min each.

for a small leakage (∼5% of initially loaded FITC-BSA) due to the quick release of FITC-BSA molecules adsorbed on the surface of particles. In the absence of laser irradiation (blue dots), the release plateaud after 3 h and remains unchanged over a period of 8 h, suggesting that no significant nonspecific release occurred and that all FITC-BSA molecules were efficiently entrapped inside the CH shell. On the other hand, if the laser was turned on for 1 min, (red dots), quick release was observed, bringing the cumulative release to 11% of the initially loaded FITC-BSA. When the laser was turned off, the release slowed quickly and reached an equilibrium value of 13% within 50 min. The drug release started again if the laser was turned back on. After 8 irradiation cycles, ∼ 92% of the initially loaded FITC-BSA was released. Furthermore, no significant leakage was observed in the absence of irradiation, suggesting a good control over drug release.

The fast drug release observed, even at low laser power densities, was possible due to the fact that all of the PhL molecules are physically located within ∼20 nm of the UCNP core, thus easing the transfer of the UV emission from the UCNPs to the photocleavable cross-links. The immediate stop of FITC-BSA release observed when the laser is turned off points to a complete control over drug release. Furthermore, complete drug release (up to 92%) can be achieved within a short time if required. All of these results suggest a fast and controllable kinetic of FITC-BSA release and prove the efficiency of the photocleavage, enabled by the fact that all of the UCNPs are individually coated with a layer of CH hydrogel containing FITC-BSA. Contrary to previous reports,[20] which involved drug release from bulk hydrogel, in this configuration the upconverted UV light from the UCNPs is efficiently used to

DOI: 10.1021/jacs.5b12357
J. Am. Chem. Soc. 2016, 138, 1078−1083

induce the photocleavage reaction in the hydrogel shell, resulting in immediate release of encapsulated drugs.

We cultured bovine nucleus (NP) cells with variable concentrations (0−500 μg/mL) of UCNPs@SiO_2@GPS@CH/PhL/FITC-BSA/PEGBA, in the presence and absence of laser irradiation to estimate the biocompatibility of this drug delivery system. The live/dead images showed that cells maintained more than 95% viability after 72 h of contact with 500 μg/mL of UCNPs@SiO_2@GPS@CH/PhL/PEGBA, exposed at the very beginning of the incubation experiment to either 9 min of continuous laser irradiation (Figure 4a) or to 5 on/off laser cycles, where the laser was on for 1 min and off for 50 min in each cycle (Figure 4b). Cells exposed to different concentrations of particles and laser irradiations maintained high cell viability (Figure S7), as well as high metabolic activity, as confirmed by the Alamar blue assay (Figure S8). These results indicate that none of the conditions significantly harmed the cells, suggesting excellent biocompatibility of this system.

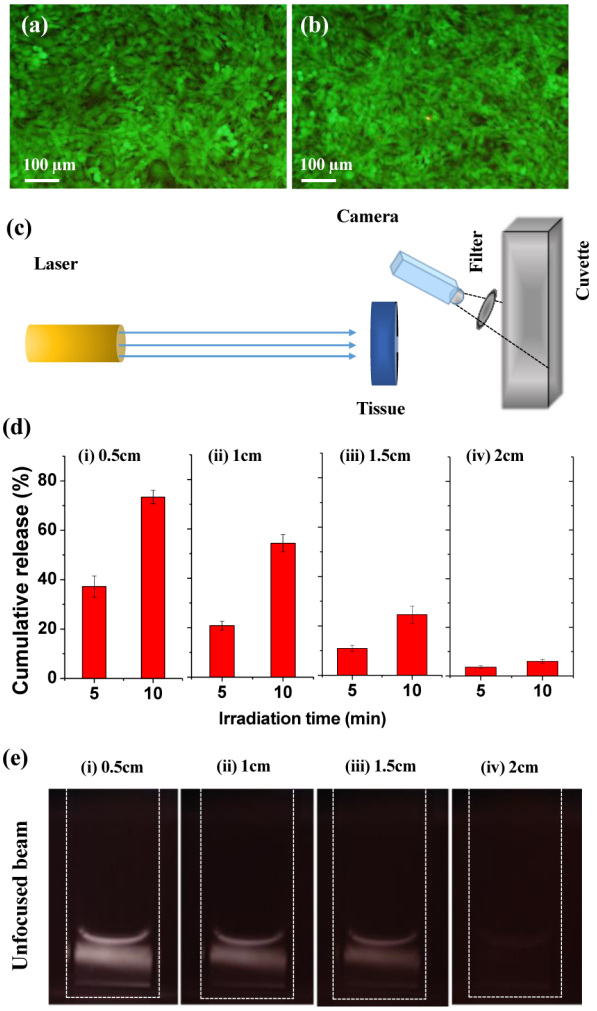

Figure 4. Combined live/dead images of NP bovine cells cultured with 500 μg/mL of UCNPs@SiO_2@GPS@CH/PhL/FITC-BSA/PEGBA and irradiated with NIR laser at a laser power density of 1.8 W/cm^2 for (a) continuous 9 min and (b) 5 on/off laser cycles; the laser was turned on for 1 min and turned off for 50 min in each cycle. (c) Schematic illustration of the experimental setup used to estimate the drug release and trackability of UCNPs inside tissues. A piece of chicken breast of varying thickness (0.5−2 cm) was placed between the laser source and the glass cuvette containing UCNPs@SiO_2@GPS@CH/PhL/FITC-BSA/PEGBA. Images are taken using a NIR camera equipped with a 775−825 nm band-pass filter. (d) Cumulative FITC-BSA release after 5 and 10 min of continuous laser irradiation at a laser power density of 1.8 W/cm^2. (e) NIR images showing upconverted NIR emission of UCNPs at 792 nm.

As observed in Figure 2d (i), the upconversion PL emission spectrum of the UCNPs contains a strong NIR peak at 792 nm, along with the peaks in Vis and UV regions. This makes Tm^{3+}/Yb^{3+} codoped UCNPs not only an excellent in situ source of UV light for phototriggered drug release but also an efficient NIR photolabel for deep tissue imaging, because the NIR emission at 792 nm is not significantly absorbed by tissues.[11,18] To assess the ability of our system to release drugs while being tracked deep inside tissues, we placed a piece of chicken tissue of varying thickness (0.5−2 cm) between the laser source and the glass cuvette containing UCNPs@SiO_2@GPS@CH/PhL/FITC-BSA/PEGBA, and used a NIR camera to collect images (Figure 4c). Using this setup, we irradiated the UCNPs continuously for a period of 5 or 10 min at a laser power density of ∼1.8 W/cm^2. The FITC-BSA release measured in the supernatant collected after centrifuging the UCNPs decreased as the thickness of tissue was increased from 0.5 to 2 cm (Figure 4d). For example, after 10 min of continuous irradiation in the presence of a 0.5 cm thick piece of tissue (Figure 4d (i)), the amount of drug released was approximately 74%, while ∼86% release was observed in the absence of tissue (Figure 3b, blue line). This release decreased to approximately 55%, 26%, and 8% when 1, 1.5, and 2 cm thick tissues were placed between the UCNPs and the laser, respectively (Figure 4d (ii)−(iv)). These results show that UCNPs can be efficiently excited as deep as 1.5 cm, and the resulting UV emission can photocleave the CH shell and release drugs; longer times would be required to release large amounts of drugs from particles placed 2 cm below the tissues, although a release that is significantly different from that due to drug leakage (Figure 3c) is observed even after only 10 min of irradiation.

The NIR-to-NIR upconversion images of the glass cuvettes containing UCNPs@SiO_2@GPS@CH/PhL/FITC-BSA/PEGBA collected with the NIR camera during laser irradiation are shown in Figure 4e. All images are filtered through a band-pass optical filter allowing only 775−825 nm light to pass through. All images showed a bright band due to the upconverted NIR emission of the particles at 792 nm. The emission intensity decreases gradually as the thickness of the tissue placed between the laser source and the glass cuvettes was increased from 0.5 to 1.5 cm. At a thickness of 2 cm, the NIR emission significantly decreased, becoming hardly distinguishable from the background (Figure 4e (iv)). A similar trend is observed if a focused laser beam is used (Figure S9).

The drug release trend shown in Figure 4d closely matched the NIR images shown in Figure 4e up to a tissue thickness of 1.5 cm. While some drug release could still be observed under 2 cm thick tissue (Figure 4d (iv)), at this depth the NIR emission was very weak. This implies that the NIR to UV upconversion is very efficient in this system, and that the limiting factor on drug release kinetics is the decreased intensity of incident light due to scattering and tissue absorption, rather than UCNP upconversion efficiency.

■ CONCLUSIONS

This is the first report that shows NIR-triggered delivery of macromolecules from UCNPs individually coated with a photocleavable hydrogel. The proposed system works under

DOI: 10.1021/jacs.5b12357
J. Am. Chem. Soc. 2016, 138, 1078−1083

low laser power and releases drugs instantaneously because all of the photocleavable moieties are present within 20 nm of the UCNP core. The drug release is immediately stopped if the laser is turned off without any significant leakage, suggesting a complete control over drug release. The dose and rate of drug release can be tuned by changing the laser power and irradiation time. The UCNP system shows excellent biocompatibility toward NP cells, which retain high metabolic activity when exposed to high concentration of UCNPs and prolonged laser irradiation. The drug release can successfully be achieved as deep as 2 cm inside tissues. Also, the NIR emission band of UCNPs at 792 nm can be used to detect particles under at least 1.5 cm thick tissues. Efficient, noninvasive, on-demand drug release and deep tissue imaging make these nanoparticles an excellent theranostic platform when localized and on-demand drug delivery is required, such as in the treatment of postsurgical wounds, localized infections, and tumors.

■ ASSOCIATED CONTENT

Supporting Information

The Supporting Information is available free of charge on the ACS Publications website at DOI: 10.1021/jacs.5b12357.

Experimental details and additional data including UV−Vis, TEM, XPS, NMR, drug release, cell viability, and PL imaging results (PDF)

■ AUTHOR INFORMATION

Corresponding Authors

*vetrone@emt.inrs.ca

*marta.cerruti@mcgill.ca

Notes

The authors declare no competing financial interest.

■ ACKNOWLEDGMENTS

We acknowledge Dr. Violeta Toader for helping with the synthesis of PhL and NMR data analysis, Dr. Marta Quintanilla for helping with PL measurements, Ms Janet Moir for cell viability assays, and Prof. Xingyi Xie for useful technical discussion. This work was supported by the Natural Sciences and Engineering Research Council of Canada (NSERC), Fonds de recherche du Québec − Nature et technologies (FRQNT), Center for Self-assembled Chemical Structures (CSACS), Canada Research Chairs (CRC), Canada Foundation for Innovation (CFI), and McGill Engineering Doctoral Award (MEDA).

■ REFERENCES

(1) Mura, S.; Nicolas, J.; Couvreur, P. *Nat. Mater.* **2013**, *12*, 991.

(2) Blum, A. P.; Kammeyer, J. K.; Rush, A. M.; Callmann, C. E.; Hahn, M. E.; Gianneschi, N. C. *J. Am. Chem. Soc.* **2015**, *137*, 2140.

(3) Qiu, Y.; Park, K. *Adv. Drug Delivery Rev.* **2012**, *64*, 49.

(4) Darwish, N.; Aragones, A. C.; Darwish, T.; Ciampi, S.; Diez-Perez, I. *Nano Lett.* **2014**, *14*, 7064.

(5) Agasti, S. S.; Chompoosor, A.; You, C. C.; Ghosh, P.; Kim, C. K.; Rotello, V. M. *J. Am. Chem. Soc.* **2009**, *131*, 5728.

(6) Kloxin, A. M.; Tibbitt, M. W.; Anseth, K. S. *Nat. Protoc.* **2010**, *5*, 1867.

(7) Carling, C. J.; Viger, M. L.; Huu, V. A. N.; Garcia, A. V.; Almutairi, A. *Chem. Sci.* **2015**, *6*, 335.

(8) Barhoumi, A.; Liu, Q.; Kohane, D. S. *J. Controlled Release*, DOI: 10.1016/j.jconrel.2015.07.018.

(9) Fomina, N.; Sankaranarayanan, J.; Almutairi, A. *Adv. Drug Delivery Rev.* **2012**, *64*, 1005.

(10) Schultz, T.; Quenneville, J.; Levine, B.; Toniolo, A.; Martinez, T. J.; Lochbrunner, S.; Schmitt, M.; Shaffer, J. P.; Zgierski, M. Z.; Stolow, A. *J. Am. Chem. Soc.* **2003**, *125*, 8098.

(11) Liu, J. A.; Bu, W. B.; Pan, L. M.; Shi, J. L. *Angew. Chem., Int. Ed.* **2013**, *52*, 4375.

(12) Yanagawa, F.; Sugiura, S.; Takagi, T.; Sumaru, K.; Camci-Unal, G.; Patel, A.; Khademhosseini, A.; Kanamori, T. *Adv. Healthcare Mater.* **2015**, *4*, 246.

(13) Griffin, D. R.; Kasko, A. M. *J. Am. Chem. Soc.* **2012**, *134*, 13103.

(14) Kloxin, A. M.; Tibbitt, M. W.; Kasko, A. M.; Fairbairn, J. A.; Anseth, K. S. *Adv. Mater.* **2010**, *22*, 61.

(15) Mackowiak, S. A.; Schmidt, A.; Weiss, V.; Argyo, C.; von Schirnding, C.; Bein, T.; Brauchle, C. *Nano Lett.* **2013**, *13*, 2576.

(16) Alexander, C. *Nat. Mater.* **2008**, *7*, 767.

(17) Coti, K. K.; Belowich, M. E.; Liong, M.; Ambrogio, M. W.; Lau, Y. A.; Khatib, H. A.; Zink, J. I.; Khashab, N. M.; Stoddart, J. F. *Nanoscale* **2009**, *1*, 16.

(18) Szacilowski, K.; Macyk, W.; Drzewiecka-Matuszek, A.; Brindell, M.; Stochel, G. *Chem. Rev.* **2005**, *105*, 2647.

(19) Chen, G.; Shen, J.; Ohulchanskyy, T. Y.; Patel, N. J.; Kutikov, A.; Li, Z.; Song, J.; Pandey, R. K.; Ågren, H.; Prasad, P. N.; Han, G. *ACS Nano* **2012**, *6*, 8280.

(20) Yang, X. J.; Liu, X.; Liu, Z.; Pu, F.; Ren, J. S.; Qu, X. G. *Adv. Mater.* **2012**, *24*, 2890.

(21) Auzel, F. *Chem. Rev.* **2004**, *104*, 139.

(22) Haase, M.; Schäfer, H. *Angew. Chem., Int. Ed.* **2011**, *50*, 5808.

(23) Bogdan, N.; Vetrone, F.; Ozin, G. A.; Capobianco, J. A. *Nano Lett.* **2011**, *11*, 835.

(24) Yan, B.; Boyer, J. C.; Branda, N. R.; Zhao, Y. *J. Am. Chem. Soc.* **2011**, *133*, 19714.

(25) Wang, W.; Liu, Q.; Zhan, C.; Barhoumi, A.; Yang, T.; Wylie, R. G.; Armstrong, P. A.; Kohane, D. S. *Nano Lett.* **2015**, *15*, 6332.

(26) Yan, B.; Boyer, J.-C.; Habault, D.; Branda, N. R.; Zhao, Y. *J. Am. Chem. Soc.* **2012**, *134*, 16558.

(27) Mahalingam, V.; Vetrone, F.; Naccache, R.; Speghini, A.; Capobianco, J. A. *Adv. Mater.* **2009**, *21*, 4025.

(28) Jalani, G.; Naccache, R.; Rosenzweig, D. H.; Lerouge, S.; Haglund, L.; Vetrone, F.; Cerruti, M. *Nanoscale* **2015**, *7*, 11255.

(29) Quintanilla, M.; Cantarelli, I. X.; Pedroni, M.; Speghini, A.; Vetrone, F. *J. Mater. Chem. C* **2015**, *3*, 3108.

DOI: 10.1021/jacs.5b12357
J. Am. Chem. Soc. 2016, 138, 1078−1083